

# Simulated vs. observed UV emission at high redshift: a hint for a clumpy ISM?

Jaime E. Forero-Romero<sup>1</sup>  $\star$ , Gustavo Yepes<sup>2</sup>, Stefan Gottlöber<sup>1</sup>, Steffen R. Knollmann<sup>2</sup>, Arman Khalatyan<sup>3</sup>, Antonio J. Cuesta<sup>4</sup>, Francisco Prada<sup>4</sup>

<sup>1</sup>*Astrophysikalisches Institut Potsdam, An der Sternwarte 16, 14482 Potsdam, Germany*

<sup>2</sup>*Grupo de Astrofísica, Universidad Autónoma de Madrid, Madrid E-28049, Spain*

<sup>3</sup>*Laboratoire d'Astrophysique de Marseille, Observatoire Astronomique de Marseille Provence,*

*Technopole de l'Étoile - Site de Chateau-Gombert, 38 rue Frédéric Joliot-Curie, 13388 Marseille Cédex 13, France*

<sup>4</sup>*Instituto de Astrofísica de Andalucía (CSIC), Camino Bajo de Huétor 50, E-18008, Granada, Spain*

22 November 2018

## ABSTRACT

We discuss the rest-frame UV emission between  $5 < z < 7$  from the *MareNostrum High-z Universe*, a SPH simulation done with more than 2 billion particles. Cosmological simulations of galaxy formation generally overpredict the UV restframe luminosity function at high redshift, both at the bright and faint ends. In this Letter we explore a dust attenuation model where a larger extinction is applied to star populations younger than a given age, mimicking the effect of a clumpy interstellar medium. We show that this scenario fits reasonably well both the UV luminosity functions and the UV-continuum slopes derived from observations. The model assumes a large obscuration for stars younger than 25 Myr from the gas clouds where they should be embedded at their formation time. We find that the optical depth in these clouds should be between 30 and 100 times larger than the mean optical depth for the homogeneous part of the interstellar medium. These values are one order of magnitude larger than those estimated in local galaxies. Therefore, we conclude that  $\Lambda$ CDM predictions for the high- $z$  UV emission can accommodate the current observations if we consider a dust extinction model based on the assumption of a clumpy environment at high redshift.

## 1 INTRODUCTION

One of the most relevant issues in cosmology is understanding the evolution of galaxy populations. Thanks to recently developed techniques and improved instrumentation, observations of high redshift galaxies ( $z > 5$ ) began to be possible during the last years (Iwata et al. 2007; Bouwens et al. 2007, 2008; McLure et al. 2009; Stark et al. 2009; Ouchi et al. 2009; Bouwens et al. 2009a,b; Oesch et al. 2009; Bunker et al. 2009; McLure et al. 2009).

The fundamental quantity used in the exploration of these galaxy populations is the galaxy luminosity function (LF). In particular, the LF in the rest-frame UV provides valuable information on key physical processes. The UV output of a galaxy imposes constraints on the instantaneous formation rate and amount of young stars in a galaxy. This kind of census provides information on the role of galactic star populations in the reionization of the Universe (Stanway et al. 2003).

Observationally, the method of choice to gather a large sample of galaxies at high redshift is the drop-out technique. This technique detects the spectral discontinuity at 912 Å (Lyman break) due to the absorption of UV radiation by in-

tergalactic hydrogen gas using multi-wavelength broad band imaging (Steidel et al. 1996). The galaxies discovered using this method receive the name of Lyman Break Galaxies (LBGs).

Motivated by the observational results, recent theoretical studies of LBGs beyond  $z > 5$  have been developed (Night et al. 2006). These theoretical studies, usually require computational techniques to produce a mock galaxy population which can be directly compared with the observed one. In the case of the rest-frame UV LF, two important elements are required in the model: the stellar population (masses, ages and metallicities) and the corresponding gas content in order to derive the extinction properties. Modelling the intrinsic UV emission through stellar population synthesis models is now a standard procedure (Maraston 1998). On the other hand, having a proper estimation of the extinction is a more uncertain process.

The estimation of the extinction can assume the form of a simple Calzetti law (Calzetti et al. 2000), where usually the UV magnitudes of each galaxy are reduced by the same amount regardless of the physical properties of the gas in the galaxy (Night et al. 2006). If the galaxy model provides information on the gas and its metallicity contents, it would

be desirable to implement a more physical model for the dust obscuration and try to put some constraints on the amount and distribution (i.e. clumpiness) of the dust on galactic scales (Inoue 2005).

In this Letter we present the first results from the *MareNostrum High-z Universe*. The simulation follows self-consistently the dynamical evolution of more than 2 billion dark matter and gas particles and includes a prescription for star formation, supernovae feedback and UV background. Here, we will present the numerical estimates for the continuum rest-frame UV emission from the stellar component, and a dust attenuation model. Our main objective is to compare the numerical predictions with the observed evolution of the UV LF between redshifts  $z = 5$  and  $z = 7$ .

## 2 SIMULATION AND GALAXY FINDING

The *MareNostrum High-z Universe* simulation<sup>1</sup> follows the non linear evolution of structures in baryons (gas and stars) and dark matter, starting from  $z = 60$  within a cube of  $50h^{-1}$ Mpc comoving on a side. The cosmological parameters used correspond to WMAP1 data (Spergel et al. 2003) and are  $\Omega_m = 0.3$ ,  $\Omega_b = 0.045$ ,  $\Omega_\Lambda = 0.7$ ,  $\sigma_8 = 0.9$ , a Hubble parameter  $h = 0.7$ , and a spectral index  $n = 1$ . The initial density field has been sampled by  $1024^3$  dark matter particles with a mass of  $m_{\text{DM}} = 8.2 \times 10^6 h^{-1} M_\odot$  and  $1024^3$  SPH gas particles with a mass of  $m_{\text{gas}} = 1.4 \times 10^6 h^{-1} M_\odot$ . The simulation has been performed using the TREEPM+SPH code GADGET-2 (Springel 2005). Radiative and Compton cooling processes for an optically thin primordial plasma of Helium and Hydrogen are included. We assumed photo-ionisation by an external spatially uniform UV-background adopting Haardt & Madau (1996). The physics of star formation is treated by means of a sub-resolution model in which the gas of the interstellar medium (ISM) is described as a multiphase medium of hot and cold gas (Yepes et al. 1997; Springel & Hernquist 2003). Stars can be formed in regions that are sufficiently dense and cold. We consider the thermal feedback of supernovae as well as the effects of stellar winds following the model described in Springel & Hernquist (2003). The gravitational smoothing scale was set to  $2 h^{-1}$ kpc in comoving coordinates. The simulation was run in the MareNostrum supercomputer using 800 processors simultaneously. This simulation is intended to study the early phases of galaxy formation. It is currently at  $z=4.55$ , after spending more than 4.5 million cpu hours.

We identify the objects in the simulations using the AMIGA Halo Finder (AHF)<sup>2</sup> which identifies both halos and subhalos. AHF is an improvement of the MHF halo finder (Gill et al. 2004), which locates local overdensities in an adaptively smoothed density field as prospective halo centers. AHF is described in detail in Knollmann & Knebe (2009).

In AHF the local potential minima are computed for each of these density peaks and the gravitationally bound particles are determined. Only peaks with at least 20 bound particles are considered as haloes and retained for further

analysis in AHF. The thermal energy of gas particles is taken into account during the calculation of the binding energy.

All objects with more than 1000 particles, dark matter, gas and stars combined, are used in our present analyses. We assume a galaxy is resolved if the object contains 200 or more star particles, which corresponds to objects with  $\gtrsim 400$  particles of gas. This ensures a proper estimation of the average gas column densities in our numerical galaxies. We then build the full Spectral Energy Distribution (SED) and compute the dust attenuation using the information from the stars and gas particles of each galaxy. In the following section we explain the details of these procedures.

## 3 SPECTRAL MODELLING

The photometric properties of the galaxies are calculated employing the stellar population synthesis model STARDUST (Devriendt et al. 1999), using the methods described in Hatton et al. (2003). We adopt a Salpeter Initial Mass Function (IMF). The SEDs are built using the AHF catalogs. Nevertheless, we have checked that all the results quoted in this Letter remain valid if we identify galaxies by the Friend-of-Friends algorithm that run over the star particles only.

The dust attenuation model parametrizes both the extinction in a homogeneous interstellar medium (ISM) and the molecular clouds around young stars, following the physical model of Charlot & Fall (2000). The attenuation from dust in the homogeneous ISM assumes later a slab geometry, while the additional attenuation for young stars assumes a spherical symmetry.

We describe first the optical depth for the homogeneous interstellar medium, denoted by  $\tau_\lambda^H$ . We take the mean perpendicular optical depth of a galactic disc at wavelength  $\lambda$  to be

$$\tau_\lambda^H = \eta \left( \frac{A_\lambda}{A_V} \right)_{Z_\odot} \left( \frac{Z_g}{Z_\odot} \right)^\tau \left( \frac{\langle N_H \rangle}{2.1 \times 10^{21} \text{ atoms cm}^{-2}} \right), \quad (1)$$

where  $A_\lambda/A_V$  is the extinction curve from Mathis et al. (1983),  $Z_g$  is the gas metallicity,  $\langle N_H \rangle$  is the mean atomic hydrogen column density and  $\eta = (1+z)^{-\alpha}$  is a factor that takes into account the evolution of the dust to gas ratio at different redshifts, with  $\alpha > 0$  from the available constraints based on simplified theoretical models (Inoue 2003) and observations around  $z \sim 3$  (Reddy et al. 2006). Given the uncertainties in this value, we will treat  $\alpha$  as a free parameter.

The mean H column density is calculated as

$$\langle N_H \rangle = X_H \frac{M_g}{m_p \pi r_g^2} \text{ atoms cm}^{-2}, \quad (2)$$

where  $X_H = 0.75$  is the universal mass fraction of Hydrogen,  $M_g$  is the mass in gas,  $r_g$  is the radius of the galaxy and  $m_p$  is the proton mass. The extinction curve depends on the gas metallicity  $Z_g$  and is based on an interpolation between the solar neighborhood and the Large and Small Magellanic Clouds ( $r = 1.35$  for  $\lambda < 2000\text{\AA}$  and  $r = 1.6$  for  $\lambda > 2000\text{\AA}$ ).

The radius, stellar and gas masses for each galaxy are taken from the AHF catalogs. Computing  $\langle N_H \rangle$  from the

<sup>1</sup> <http://astro.ft.uam.es/marenostrum>

<sup>2</sup> It is a MPI+OpenMP hybrid halo finder to be downloaded freely from <http://www.popia.ft.uam.es/AMIGA>

galaxy catalogs turns out to give similar results, on average, than integrating the 3D gas distribution of the galaxies using the appropriate SPH kernel. The difference between the average Hydrogen column densities calculated in these two different ways are less than 15% regardless of the size of the galaxy, provided that the gas distribution is sampled with more than 200 particles.

In addition to the foreground, homogeneous ISM extinction, we also model, in a simple manner, the attenuation of young stars that are embedded in their nest clouds. Stars younger than a given age,  $t_c$ , are subject to an additional attenuation with mean perpendicular optical depth

$$\tau_\lambda^C = \left(\frac{1}{\mu} - 1\right) \tau_\lambda^H, \quad (3)$$

where  $\mu$  is the fraction of the total optical depth seen by the young stars that is found in the homogeneous ISM. Kong et al. (2004) in a study of 115 nearby galaxies, spanning a wide range of star formation activities, find that  $\mu$  is typically  $\sim 1/3$  with a wide range of scatter between 0.1 and 0.6. Given the possible uncertainties in extrapolating the typical values of  $\mu$  to high redshift, we will treat this quantity as a free parameter.

#### 4 ANALYSIS AND RESULTS

In the calculation of the luminosity functions we have made first an additional correction motivated from the different abundance of dark matter halos between the cosmology used in the simulation (WMAP1,  $\sigma_8 = 0.90$  (Spergel et al. 2003)) and the values of the cosmological parameters estimated from the latest CMB results (WMAP5,  $\sigma_8 = 0.796$  (Dunkley et al. 2009)). At a given redshift and mass range, the WMAP1 universe has a larger halo number density than in the WMAP5 one. We estimate the influence of a different cosmology using the Sheth-Tormen formalism (Sheth & Tormen 1999). The ratio between the WMAP5 and WMAP1 halo mass functions is used as a weight factor for each galaxy (depending on the mass of the host halo) in the construction of the LF. This procedure is justified because of the strong correlation shown between the UV luminosity and the halo mass.

We have tested this correction by running two additional simulations with exactly the same mass and force resolutions but a corresponding smaller volume to speed up the calculations (i.e  $2 \times 256^3$  particles in a  $12.5 h^{-1}$  Mpc comoving boxsize). They were performed with same initial conditions using the WMAP1 and WMAP5 cosmological parameters. Though not shown here, we do reproduce the results of the WMAP5 run when using the WMAP1 run with the aforementioned correction.

The results after correcting for the halo abundance are shown in Figure 1. The black squares represent the results without any dust extinction. All the rest-frame UV LFs, without dust extinction, strongly over-predict (up to 2 orders of magnitude) the observational estimates in all the redshift range, in fairly agreement with results from other  $\Lambda$ CDM simulations (Night et al. 2006).

This discrepancy cannot be attributed to the selection of the Salpeter IMF to compute the SEDs. Other IMFs,

such as Chabrier (Chabrier 2003) or Kroupa (Kroupa 2001) have lower mass to luminosity ratios in the UV (at most  $\sim 1.5$ ) with respect to a Salpeter IMF, for a young starburst of a given age. (Chabrier 2003; Bruzual & Charlot 2003). These IMFs would then increase the discrepancy between our simulation and observations.

One could argue that the excess of galaxies in our simulation could be related with some of the astrophysical processes that shape the luminosity function at low redshift (Benson et al. 2003). In particular, an improved modelling of supernovae and quasar feedbacks can modify the luminosity function. This scenario cannot be ruled out on the basis of the present simulation, and certainly deserves further study. Nevertheless, in our case, we want to show that a simple, physically motivated extinction model can explain the different behaviour of the simulated and observed UV LF.

If we apply only the extinction due to the homogeneous ISM, parametrized by  $\mu = 1.0$  (for any value of  $\alpha$ ) then only the most massive galaxies are effectively extinguished. If we modify the values of  $\alpha$  in such a way as to match the bright end of the observed LF, we still find an excess of simulated galaxies at the faint end. To modify the luminosities at the faint end, specially at  $z = 5$  and  $z = 6$ , one needs to apply a larger extinction on the young stars. The correction on the population of young stars turns out to be independent on the total mass of the galaxy, modifying both the bright and faint ends of the LFs.

We explore the parameter space in order to find the best set of parameters ( $\alpha$ ,  $\mu$ ,  $t_c$ ) in our extinction model which provides a good fit to the observational data. In Figure 1 the red hexagons show the results for the best fit parameters:  $\alpha = 1.5$ ,  $\mu = 0.01 - 0.03$  and  $t_c = 25$  Myr. It means that stars younger than  $t_c = 25$  Myr are almost completely extinguished. Thus, the optical depth in the clouds embedding the young stars must be between 30 ( $\mu = 0.03$ ) and 100 ( $\mu = 0.01$ ) times larger than the optical depth in the ISM. For comparison, the largest values found in local galaxies by Kong et al. (2004) are  $\sim 10$  times the optical depth in the ISM. Furthermore, we do not find any strong degeneracy between the parameters  $\alpha$  and  $\mu$ .

We consider now the colors of the galaxies. One of the simplest ways to observationally estimate the dust attenuation is through the UV slope  $\beta$  ( $f_\lambda \propto \lambda^\beta$ ). In Figure 2 we show the values for  $\beta$  in the simulated galaxies and compared to recent observational estimations (Bouwens et al. 2009,b). We find that that the extinguished colors are consistent with the constraints worked out from the observations. There is a minor discrepancy at the faintest magnitudes ( $M_{AB} \sim -19$ ) which is not highly significant if we consider that the error bars in the Figure 2 represent a  $1-\sigma$  scatter. Remarkably, some extinguished simulated galaxies at  $z \sim 7$  (not shown in the Figure) still show very blue slopes  $\beta \sim 3$  as seen in the observations.

#### 5 CONCLUSIONS

We have used the *MareNostrum High- $z$  Universe*, currently the largest SPH simulation of galaxy formation, with more than 2 billion particles, to study the evolution of the rest-frame UV luminosity function between  $5 < z < 7$ . We find

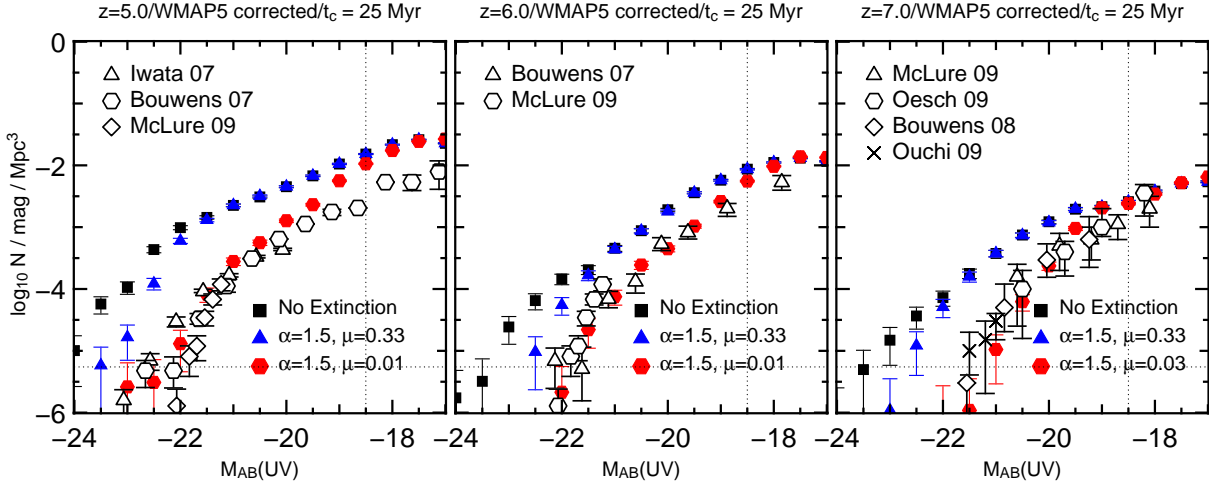


**Figure 1.** Luminosity functions at redshifts  $z \sim 5, 6$  and  $7$ . The error bars are poissonian. The horizontal line shows the limits of one object per unit magnitude in the simulation volume, for the used bin size  $\Delta M_{AB} = 0.50$ . The vertical line indicates the approximate limit for well resolved objects following a criteria of more than 200 star particles. This limit corresponds to similar UV magnitudes at every redshift. The simulation data has been already corrected for the different abundance of dark matter halos between the WMAP1 and WMAP5 cosmologies. The open symbols represent the observations. The filled symbols represent different extinction prescriptions on the simulated galaxies: no extinction (black squares), homogeneous ISM plus an intermediate extinction on young stars (blue triangles) and a extreme extinction on young stars (red hexagons). In the model with extreme extinction on young stars, all the stars younger than 25 Myr are almost completely extinguished.

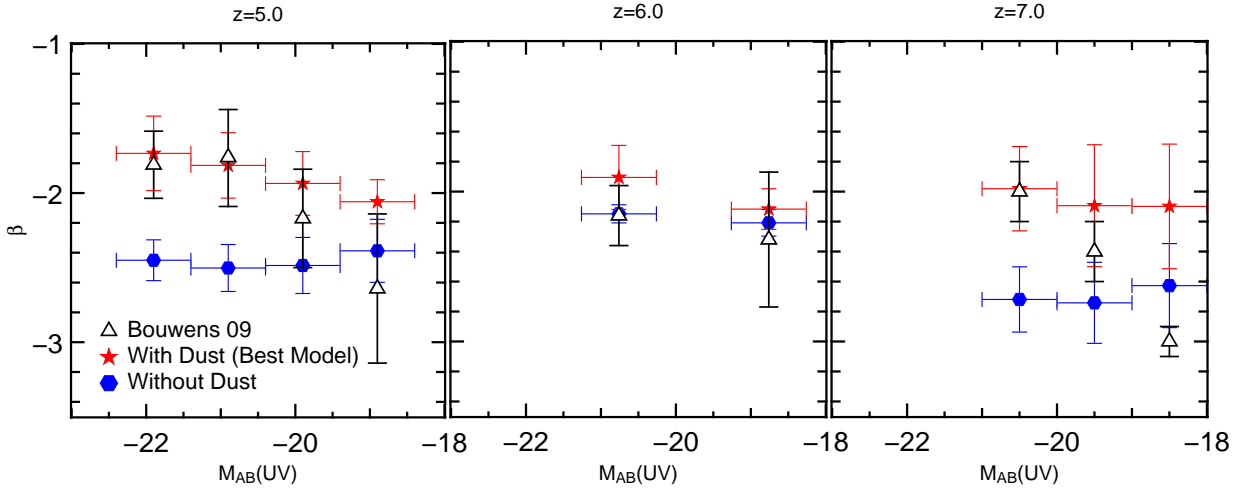


**Figure 2.** The slope,  $\beta$ , of the UV-continuum versus absolute UV magnitudes of simulated galaxies at  $z \sim 5, 6$  and  $7$ . The blue points correspond to the  $\beta$  determinations without extinction, red points correspond to the estimation with the extinction model consistent with the UV luminosity functions. The open symbols represent the estimated values of  $\beta$  from HST observations. In both cases the vertical error bars represent a  $1\text{-}\sigma$  scatter. The brightest galaxies in the simulation follows the same color trend as in observations. Some discrepancy is still present at the faint end though.

that the UV LF from the simulation over-predicts systematically the observations. Using a Chabrier, Kroupa or Top Heavy IMF, instead of the Salpeter IMF we have used here, will increase the disagreement.

We further correct the luminosity of each galaxy by dust attenuation. If we correct only by the attenuation produced by an homogeneous ISM, with an optical depth calculated using Equation 1, we find that the results are unsatisfactory. In that kind of extinction model, the dust optical depth turns out to be dependent on the mass of the galaxy, making

the bright end of the LF more extinguished than the faint end, the latter remaining basically unchanged.

We use then a simple but physically motivated model based on Charlot & Fall (2000), where the extinction is described by a homogeneous ISM component plus a clumpy component affecting the younger stars. We find that the additional extinction on the younger stars is necessary to reproduce the overall normalization and shape of the luminosity functions between  $5 < z < 7$ . The final modification on the UV luminosities is independent on the total mass of

the galaxy, meaning that the faint end of the LF can be modified as well.

We find that all the stars younger than 25 Myr must be obscured almost completely in order to get a good agreement to the observed evolution of the LFs. This means that the optical depth in the clouds embedding the young stars must be between 30 and 100 times larger than the optical depth from the homogeneous ISM. Compared to observations of local galaxies this proportion between the two optical depths is one order of magnitude larger than the highest estimates. The agreement of our model to available observational constraints hints for a clumpy ISM at high redshift.

The extinction model we propose is consistent with the observational constraints of the UV slope between  $5 < z < 7$ . We even find some galaxies with very blue UV slopes as seen in galaxies at  $z \sim 7$  (Bouwens et al. 2009b). The agreement is less satisfactory at lower UV magnitudes  $M_{AB} \sim -19$ . The extinction model we apply to the very young stars is thus not visible as a strong change in the UV slopes, but could be observationally detected in the rest-frame infrared with instruments like HERSCHEL and ALMA. A complementary view of the results presented so far will be provided in an upcoming publication on the physical nature of Lyman- $\alpha$  Emitters in the *MareNostrum High-*z* Universe*.

## ACKNOWLEDGMENTS

The simulation used in this work is part of the MareNostrum Numerical Cosmology Project at the BSC. The data analysis has been performed at the NIC Jilich and at the LRZ Munich. We acknowledge the LEA Astro-PF collaboration and the ESF ASTROSIM network for financial support. J.E.F.-R., S.G. and A.K. acknowledge support by DAAD through the PROCOPE program. A.K. acknowledges support from ANR-06-BLAN-0172. G.Y. acknowledges support from MEC projects FPA2006-01105 and AYA2006-15492-C03.

## REFERENCES

- Benson A. J., Bower R. G., Frenk C. S., Lacey C. G., Baugh C. M., Cole S., 2003, *ApJ*, 599, 38
- Bouwens R. J., Illingworth G. D., Franx M., Chary R., Meurer G. R., Conselice C. J., Ford H., Giavalisco M., van Dokkum P., 2009, *ArXiv e-prints*
- Bouwens R. J., Illingworth G. D., Franx M., Ford H., 2007, *ApJ*, 670, 928
- Bouwens R. J., Illingworth G. D., Franx M., Ford H., 2008, *ApJ*, 686, 230
- Bouwens R. J., Illingworth G. D., Oesch P. A., Stiavelli M., van Dokkum P., Trenti M., Magee D., Labbe I., Franx M., Carollo M., 2009, *ArXiv e-prints*
- Bouwens R. J., Illingworth G. D., Oesch P. A., Trenti M., Stiavelli M., Carollo M., Franx M., van Dokkum P. G., Labbe I., Magee D., 2009, *ArXiv e-prints*
- Bruzual G., Charlot S., 2003, *MNRAS*, 344, 1000
- Bunker A., Wilkins S., Ellis R., Stark D., Lorenzoni S., Chiu K., Lacy M., Jarvis M., Hickey S., 2009, *ArXiv e-prints*
- Calzetti D., Armus L., Bohlin R. C., Kinney A. L., Koornneef J., Storchi-Bergmann T., 2000, *ApJ*, 533, 682
- Chabrier G., 2003, *PASP*, 115, 763
- Charlot S., Fall S. M., 2000, *ApJ*, 539, 718
- Devriendt J. E. G., Guiderdoni B., Sadat R., 1999, *A&A*, 350, 381
- Dunkley J., Komatsu E., Nolta M. R., Spergel D. N., Larson D., Hinshaw G., Page L., Bennett C. L., Gold B., Jarosik N., Weiland J. L., Halpern M., Hill R. S., Kogut A., Limon M., Meyer S. S., Tucker G. S., Wollack E., Wright E. L., 2009, *ApJS*, 180, 306
- Gill S. P. D., Knebe A., Gibson B. K., 2004, *MNRAS*, 351, 399
- Haardt F., Madau P., 1996, *ApJ*, 461, 20
- Hatton S., Devriendt J. E. G., Ninin S., Bouchet F. R., Guiderdoni B., Vibert D., 2003, *MNRAS*, 343, 75
- Inoue A. K., 2003, *PASJ*, 55, 901
- Inoue A. K., 2005, *MNRAS*, 359, 171
- Iwata I., Ohta K., Tamura N., Akiyama M., Aoki K., Ando M., Kiuchi G., Sawicki M., 2007, *MNRAS*, 376, 1557
- Knollmann S. R., Knebe A., 2009, *ApJS*, 182, 608
- Kong X., Charlot S., Brinchmann J., Fall S. M., 2004, *MNRAS*, 349, 769
- Kroupa P., 2001, *MNRAS*, 322, 231
- Maraston C., 1998, *MNRAS*, 300, 872
- Mathis J. S., Mezger P. G., Panagia N., 1983, *A&A*, 128, 212
- McLure R. J., Cirasuolo M., Dunlop J. S., Foucaud S., Almaini O., 2009, *MNRAS*, 395, 2196
- McLure R. J., Dunlop J. S., Cirasuolo M., Koekemoer A. M., Sabbi E., Stark D. P., Targett T. A., Ellis R. S., 2009, *ArXiv e-prints*
- Night C., Nagamine K., Springel V., Hernquist L., 2006, *MNRAS*, 366, 705
- Oesch P. A., Bouwens R. J., Illingworth G. D., Carollo C. M., Franx M., Labbe I., Magee D., Stiavelli M., Trenti M., van Dokkum P. G., 2009, *ArXiv e-prints*
- Ouchi M., Mobasher B., Shimasaku K., Ferguson H. C., Fall M. S., Ono Y., Kashikawa N., Morokuma T., Nakajima K., Okamura S., Dickinson M., Giavalisco M., Ohta K., 2009, *ArXiv e-prints*
- Reddy N. A., Steidel C. C., Fadda D., Yan L., Pettini M., Shapley A. E., Erb D. K., Adelberger K. L., 2006, *ApJ*, 644, 792
- Sheth R. K., Tormen G., 1999, *MNRAS*, 308, 119
- Spergel D. N., Verde L., Peiris H. V., Komatsu E., Nolta M. R., Bennett C. L., Halpern M., Hinshaw G., Jarosik N., Kogut A., Limon M., Meyer S. S., Page L., Tucker G. S., Weiland J. L., Wollack E., Wright E. L., 2003, *ApJS*, 148, 175
- Springel V., 2005, *MNRAS*, 364, 1105
- Springel V., Hernquist L., 2003, *MNRAS*, 339, 289
- Stanway E. R., Bunker A. J., McMahan R. G., 2003, *MNRAS*, 342, 439
- Stark D. P., Ellis R. S., Bunker A., Bundy K., Targett T., Benson A., Lacy M., 2009, *ApJ*, 697, 1493
- Steidel C. C., Giavalisco M., Dickinson M., Adelberger K. L., 1996, *AJ*, 112, 352
- Yepes G., Kates R., Khokhlov A., Klypin A., 1997, *MNRAS*, 284, 235